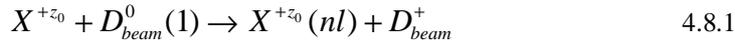# ADAS308: Charge exchange spectroscopy - process effective coefficients: l-resolved
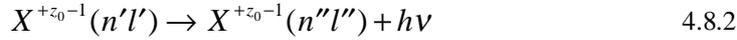
The program analyses *column* (line-of-sight integrated) emissivity observations of charge exchange spectroscopy lines from hydrogenic impurities, occuring through neutral beam / plasma interaction, in terms of emission measure. It predicts the column intensities of spectral components of the charge exchange lines, the Doppler broadened line shapes and effective emission coefficients for arbitrary lines in an l-resolved picture.
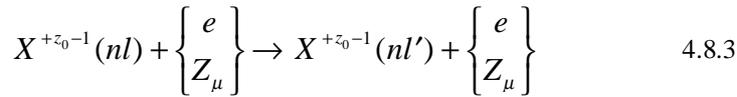
## Background theory:

Charge exchange spectroscopy is driven by reactions of the form

$$X^{+z_0} + D_{beam}^0(1) \rightarrow X^{+z_0}(nl) + D_{beam}^+ \qquad 4.8.1$$

in which an electron is captured from a donor atom in its ground (or an excited) state. The principal application is usually to capture by the bare nuclei of impurity atoms in the plasma from the ground state of deuterium, helium or lithium atoms in fast neutral beams. Subsequently the hydrogen-like impurity ion radiates as

$$X^{+z_0-1}(n'l') \rightarrow X^{+z_0-1}(n''l'') + h\nu \qquad 4.8.2$$

Composite spectral line features of the form $n' \rightarrow n''$ are observed made up from unresolved $n'l' \rightarrow n''l''$ multiplet components. Charge exchange line features often involve high principal quantum shells and occur over wide spectral ranges including the visible range. In general the populations of receiver levels are modified by redistributive collisions with plasma ions and electrons and by fields before radiation emission occurs. The present programme includes redistributive collisions of the form

$$X^{+z_0-1}(nl) + \begin{Bmatrix} e \\ Z_\mu \end{Bmatrix} \rightarrow X^{+z_0-1}(nl') + \begin{Bmatrix} e \\ Z_\mu \end{Bmatrix} \qquad 4.8.3$$

where $Z_\mu$ denotes a bare nucleus of charge $Z_\mu$ and field induced redistribution of the form

$$X^{+z_0-1}(nl) \underset{B_{mag}}{\rightarrow} X^{+z_0-1}(nl') \qquad \text{[ not fully implemented]} \quad 4.8.4$$

The line-of-sight integrated photon emissivity of a charge exchange driven line may be written as

$$
\begin{aligned}
I_{n \rightarrow n'}^{(z_0-1)} &= \sum_{l,l'} I_{nl \rightarrow n'l'}^{(z_0-1)} \\
&= \int_S \sum_{l,l'} A_{nl \rightarrow n'l'} N_{nl}^{(z_0-1)} ds \\
&= \int_S [\sum_{l,l'} A_{nl \rightarrow n'l'} (N_{nl}^{(z_0-1)} / N_D N^{(z_0)})] N_D N^{(z_0)} ds \\
&= \int_S [\sum_{l,l'} q_{nl \rightarrow n'l'}^{(eff)}] N_D N^{(z_0)} ds \\
&= \int_S q_{n \rightarrow n'}^{(eff)} N_D N^{(z_0)} ds \\
&\approx q_{n \rightarrow n'}^{(eff)} \int_S N_D N^{(z_0)} ds
\end{aligned}
\qquad 4.8.5
$$

where $S$ is the path length through the neutral beam / plasma intersection along a spectrometer line-of-sight. $N_D$ is the neutral donor number density and $N^{(z_0)}$ is the number density of fully ionised impurity atoms. $q_{n \rightarrow n'}^{(eff)}$ is the *effective emission*

*coefficient* for the whole $n \to n'$ principal quantum shell transition and $\int_S N_D N^{(z_0)} ds$ is the *emission measure*. The mean transition energy is

$$\Delta E_{n,n'} = (\sum_{l,l'} \Delta E_{nl,n'l'} q_{nl \to n'l'}^{(eff)}) / q_{n \to n'}^{(eff)} \qquad 4.8.6$$

where $\Delta E_{nl,n'l'}$ is the line component transition energy and $q_{nl \to n'l'}^{(eff)}$ is the component effective emission coefficient. The effective emission coefficient $q_{n \to n'}^{(eff)}$ may be calculated theoretically. If it is approximately constant over the emitting volume, then measurement of a charge exchange line intensity $I_{n \to n'}^{(z_0-1)}$ allows deduction of the emission measure $\int_S N_D N^{(z_0)} ds$. If neutral beam attenuation to the observed volume is known or calculable then local impurity density may be inferred.

*Relationship to direct coefficients*:
With the effective emission coefficients calculated theoretically, comparison with one observed charge exchange line intensity allows deduction of the emission measure. Then all other line intensities are predictable. If more than one line intensity is observed, then a mean emission measure may be deduced and some comment may be made on the ratios of exeperimental to theoretical effective emission coefficients. The organisation of the collisional-radiative modelling in ADAS308 is specifically designed to allow such comparison. The following points and assumptions are made:
(i) From the theoretical point-of-view the direct capture cross-sections to levels are more fundamental quantities for comparison with experiment that the effective emission coefficients.
(ii) The dominant fundamental processes modifying the initial distribution of capture are redistribution within an *n*-shell and radiative cascade in low and moderate density plasmas. Limiting the collisional-radiative theory to these dominant processes allows a compact invertable relationship to be established between column emissivities of charge exchange spectrum lines and direct capture cross-sections.
(ii) It is of most practical value to target experiment / theory comparisons on the *n*-shell distribution of capture (including the *n*-shell decrement) in fusion studies. This may be achieved by imposing theoretical information on the *l* sub-shell distribution of capture.

Consider the monoenergetic direct capture rate coefficients to *nl* sub-levels $q_{nl}^{(CX)}$ from the initial neutral donor state $D^0(1)$ by the fully stripped impurity ion with number density $N^{(z_0)}$, denoted more compactly by $N^+$.

$$q_{nl}^{(CX)}(E_u) = v \, \sigma_{nl}^{(CX)}(v) \qquad 4.8.7$$

where $E_u$ is the relative collision energy per atomic mass unit so that $v = \sqrt{2E_u / m_p}$ is the relative collision speed, with $m_p$ the proton mass and $\sigma$ the capture cross-section.
It is supposed that

$$q_{nl}^{(CX)}(E_u) = f_{(n)l}^{(theor)} q_n^{(CX)}(E_u) \qquad 4.8.8$$

Since no collisional excitation from lower to higher *n*-shells is allowed, the populations of the *lj* sublevels of the principal quantum shell $n' \geq n+1$ may be written as

$$N_{n'l'} = N_D N^+ \sum_{n^{iv} \geq n+1} W_{n'l',n^{iv}} q_{n^{iv}}^{(CX)} \qquad 4.8.9$$

Then the equations determining the populations of the sub-shells of the principal quantum shell *n* are

$$\sum_{l''} M_{(n)l,l''} N_{nl''} = N_D N^+ f_{(n)l}^{(theor)} q_n^{(CX)} + \sum_{n' \geq n+1} A_{nl,n'l'} N_{n'l'} \qquad 4.8.10$$

so that

$$N_{nlj} = N_D N^+ W_{nlj,n} q_n^{(CX)} + N_D N^+ \sum_{n^{iv} \geq n+1} W_{nlj,n^{iv}} q_{n^{iv}}^{(CX)} \qquad 4.8.11$$

with

$$W_{nlj,n} = [\sum_{l''j''} M_{(n)lj,l''j''}^{-1} f_{(n)l''j''}^{(theor)}] q_n^{(CX)} \qquad 4.8.12$$

and

$$W_{nlj,n^{iv}} = \sum_{l'',j'',l',j'} M_{(n)lj,l''j''}^{-1} A_{nl''j'',n'l'j'} W_{n'l'j',n^{iv}} \qquad 4.8.13$$

The solution can proceed recursively downwards in $n$ with compact vector and array storage.

Tabulations of experimental or theoretical state selective charge exchange cross-section data span a range of principal quantum shells $\sigma_{nlj}^{(CX)}(v): n_0 \leq n \leq n_1$. Cascade from levels $n > n_1$ may contribute significantly to the populations of lower levels especially at high collision energies when the decrease of the direct charge exchange cross-sections with $n$ is slow ($\sigma_n \sim n^{-\alpha}$ and $\alpha \sim 3$). However, redistribution amongst $lj$ sub-levels of the higher $n$-shells is high, approaching statistical in most circumstances. Therefore the cascade solution is initiated at some $n_{max}$ (~20 typically) for complete $n$-shell populations only (matrices $W^{(high)}$), with subshells implicitly statistically populated, down to $n_1$ whereupon the $lj$ resolved solution (matrices $W^{(low)}$) is commenced.

In general observable spectrum lines are associated with upper principal quantum shells $n \leq n_1$. If $M_{rep}$, lines are identified each with a distinct upper $n$-shells $\bar{n}_{irep}: irep = 1, \ldots, M_{rep}$, then a 'condensation' may be imposed such that

$$q_n^{(CX)} = \sum_{irep=1}^{M_{rep}} L_{n,irep} q_{\bar{n}_{irep}}^{(CX)} \qquad \text{for } n_0 \leq n \leq n_1 \qquad 4.8.14$$

and

$$q_n^{(CX)} = (n/n_1)^{\alpha} q_{n_1}^{(CX)} \qquad \text{for } n > n_1 \qquad 4.8.15$$

giving, after integration along the line-of-sight, a matrix relation

$$\begin{bmatrix} I_{\bar{n}_1 \to \bar{n}_1'} \\ . \\ I_{\bar{n}_{M_{rep}} \to \bar{n}_{M_{rep}}'} \end{bmatrix} = (\int_S N_D N^+ ds) \begin{bmatrix} a_{11} & . & a_{1M_{rep}} \\ . & . & . \\ a_{M_{rep}1} & . & a_{M_{rep}M_{rep}} \end{bmatrix} \begin{bmatrix} q_{\bar{n}_1}^{(CX)} \\ . \\ q_{\bar{n}_{M_{rep}}}^{(CX)} \end{bmatrix}$$

$$4.8.16$$

The coefficients of the matrix are theoretically calculated quantities. The equations may be solved for the the $q_{\bar{n}_i}^{(CX)}$ and the emission measure $\int_S N_D N^+ ds$ subject to the constraint

$$\sum_{irep=1}^{M_{rep}} q_{\bar{n}_{irep}}^{(CX)} = \sum_{irep=1}^{M_{rep}} q_{\bar{n}_{irep}}^{(CX)(theor)} \qquad 4.8.17$$

*Energy levels*:
Precise energy levels are required in calculating collisional redistribution between the degenerate and nearly degenerate states. This is also required in reconstructing precise *n-n'* line feature shapes. The cases of hydrogen-like ions and lithium-like ions are treated separately

*Case(i): hydrogen-like ions*

$$E(nl\ ^2L_{l+1/2}) = -(z_{eff\,1}^2 / n^2)I_H - RMC_{nl}(z_{eff\,2})$$
$$+ \tfrac{1}{2}l\ ZETA_{nl}(z_{eff\,2}) + \delta_{l,0}QED_n(z_{eff\,2})$$
$$E(nl\ ^2L_{l-1/2}) = -(z_{eff\,1}^2 / n^2)I_H - RMC_{nl}(z_{eff\,2})$$
$$+ \tfrac{1}{2}(l+1)\ ZETA_{nl}(z_{eff\,2}) \qquad 4.8.18$$

where

$$RMC_{nl}(z) = \begin{cases} (\alpha^2 z^4 / n^4)[(n/l+\tfrac{1}{2}) - \tfrac{3}{4}]I_H & l > 0 \\ (\alpha^2 z^4 / n^4)[(n/l+1) - \tfrac{3}{4}]I_H & l = 0 \end{cases}$$

$$ZETA_{nl}(z) = \begin{cases} (2\alpha^2 z^4 / n^4)[n/l(2l+1)(l+1)]I_H & l > 0 \\ 0 & l = 0 \end{cases}$$
$$4.8.19$$

$$QED_n(z) = (8\alpha^3 z^4 / 3\pi n^3)\{\ln[1/(\alpha z)^2] + \tfrac{19}{30} + L_n\}I_H$$

with $L_1$=-2.984128, $L_2$=4.811768, $L_3$=-2.767699, $L_4$=-2.749859 and $L_n$=-2.71632-0.02402(5/n)$^{3/2}$ . The effective charge prescription is $z_{eff1} = z_{eff2} = z_0$.

*Case (ii): lithium-like ions*

$$E(1s^2nl\ ^2L_{l+1/2}) = E^{Edlen}(z_{eff\,1}) + \tfrac{1}{2}l\ ZETA_{nl}(z_{eff\,2})$$
$$E(1s^2nl\ ^2L_{l-1/2}) = E^{Edlen}(z_{eff\,1}) + \tfrac{1}{2}(l+1)\ ZETA_{nl}(z_{eff\,2})\ \ 4.8.20$$

where the $E^{Edlen}$ are obtained from Ritz formulae for $s$ and $p$ orbitals and from polarisabilities for $l > 1$ due to Edlen (1979). The effective charge prescription is $z_{eff1} = z_0, z_{eff2} = z_0$-2.

*Alternate driving processes*:
Primary fundamental state selective charge exchange cross-section data for the calculations are taken from ADAS compilations (type ADF01) in general. For contrast, a calculation may be carried out using state selective cross-sections from analytic expressions in the high energy Eikonal approximation. These analystic expressions are available for 1s, 2sand 2p donor states of neutral hydrogen and for the $1s^2$ and 1s2s states of neutral helium. It is of interest to compare the analysis with that which would occur with two alternative driving mechanisms. These are free electron capture and collisional excitation by electron impact from the ground state of the hydrogen-like impurity ion. The previous formulation remains the same but with the emission measure and capture rate coefficients redefined as

$$\int_S N_e N^+ ds \qquad \text{and} \qquad q_{\bar{n}_i}^{(rec)} \qquad\qquad 4.8.21$$

or

$$\int_S N_e N^{(z_0-1)}(1s)ds \qquad \text{and} \qquad q_{1\to\bar{n}_i}^{(exc)} \qquad\qquad 4.8.22$$

respectively.

*Source data* :
The program operates on collections of fundamental state selective charge exchange cross-section data. The allowed content, organisation and formatting of these files are specified in ADAS data format ADF01. Centrally supported data collections are stored in directories such as

     */.../adas/adas/adf01/qcx#h0/*

where the *h0* identifies neutral hydrogen is the donor. The individual data set names take the form
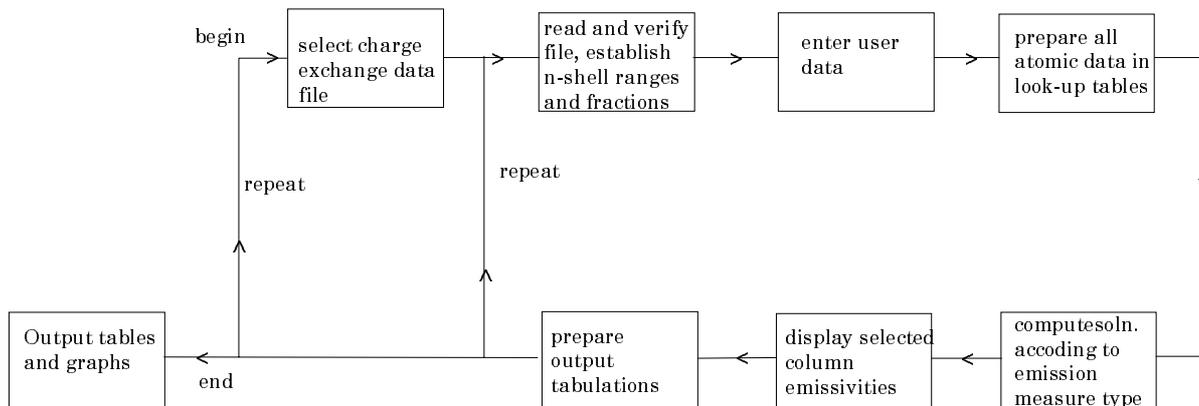
     *qcx#h0_<code>.#<ion>.dat*

where <code> is a three character identifier of the source and <ion> is the receiving fully ionised ion (for example *c6*). More detail is given below.

# Program steps:

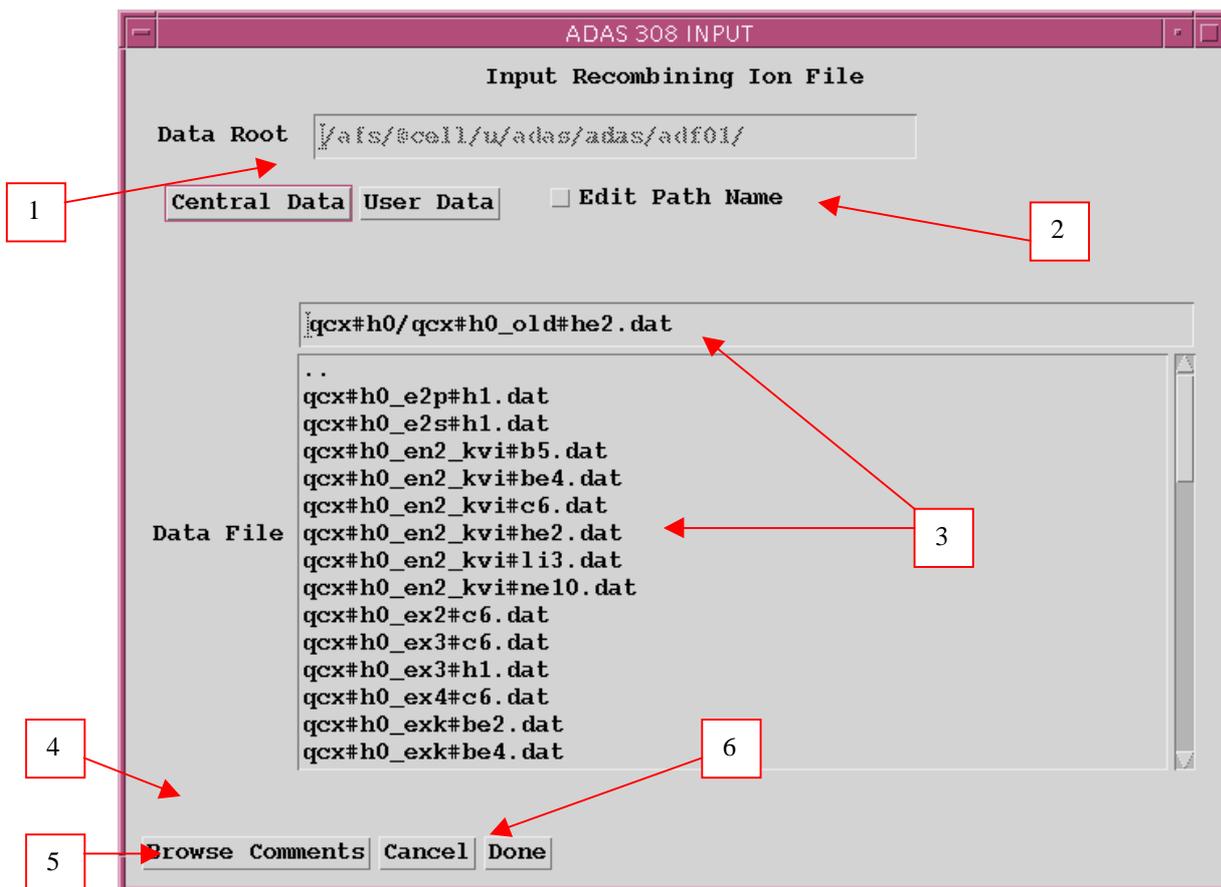These are summarised in the figure below.

Figure 4.8



# Interactive parameter comments:

ADAS308, which make use of data from archived ADAS datasets, initiates an interactive dialogue with the user in three parts, namely, input file selection, entry of user data and disposition of output.

The **file selection window** is shown below.

1.  Data root shows the full pathway to the appropriate data subdirectories. Click the *Central Data* button to insert the default central ADAS pathway to the correct data type – ADF01 in this case. Note that each type of data is stored according to its ADAS data format (*adf* number). Click the *User Data* button to insert the pathway to your own data. Note that your data must be held in a similar file structure to central ADAS, but with your identifier replacing the first *adas,* to use this facility.
2.  The Data root can be edited directly. Click the *Edit Path Name* button first to permit editing.
3.  Available sub-directories are shown in the large file display window. Scroll bars appear if the number of entries exceed the file display window size. There are a large number of these. They are stored in sub-directories by donor which is usually neutral but not necessarily so (eg. *qcx#h0*). The individual members are identified by the subdirectory name, a code and then fully ionised receiver (eg. qcx#h0_*old#c6.dat*). The data sets generally contain *nl*-resolved cross-section data but *n*-resolved and *nlm*-resolved are handled. Resolution levels must not be mixed in datasets. The ADF01 file nmaes distinguish different sources. The first letter *o* or the code *old* has been used to indicate that the data has been produced from JET compilations which originally had parametrised *l*-distribution of cross-sections. The nl-resolved data with such code has been reconstituted from them. Data of code *old* is the preferred JET data. Other sources codes include *ory* (old Ryufuku), *ool* (old Olson), *ofr* (old Fritsch) and *omo* (old molecular orbital). There are newer data such as *kvi*. Additional codes are used for excited donors such as *ex2* for hydrogen n=2. Click on a name to select it. The selected name appears in the smaller selection window above the file display window. Then the individual datafiles are presented for selection. Datafiles all have the termination *.dat*.
4.  Once a data file is selected, the set of buttons at the bottom of the main window become active.

**ADAS 308 INPUT**

**Input Recombining Ion File**

Data Root  `/afs/#cell/u/adas/adas/adf01/`

1

Central Data  User Data       ☐ Edit Path Name

2

`qcx#h0/qcx#h0_old#he2.dat`

3

```
..
qcx#h0_e2p#h1.dat
qcx#h0_e2s#h1.dat
qcx#h0_en2_kvi#b5.dat
qcx#h0_en2_kvi#be4.dat
qcx#h0_en2_kvi#c6.dat
Data File  qcx#h0_en2_kvi#he2.dat
qcx#h0_en2_kvi#li3.dat
qcx#h0_en2_kvi#ne10.dat
qcx#h0_ex2#c6.dat
qcx#h0_ex3#c6.dat
qcx#h0_ex3#h1.dat
qcx#h0_ex4#c6.dat
qcx#h0_exk#be2.dat
qcx#h0_exk#be4.dat
```

4

6

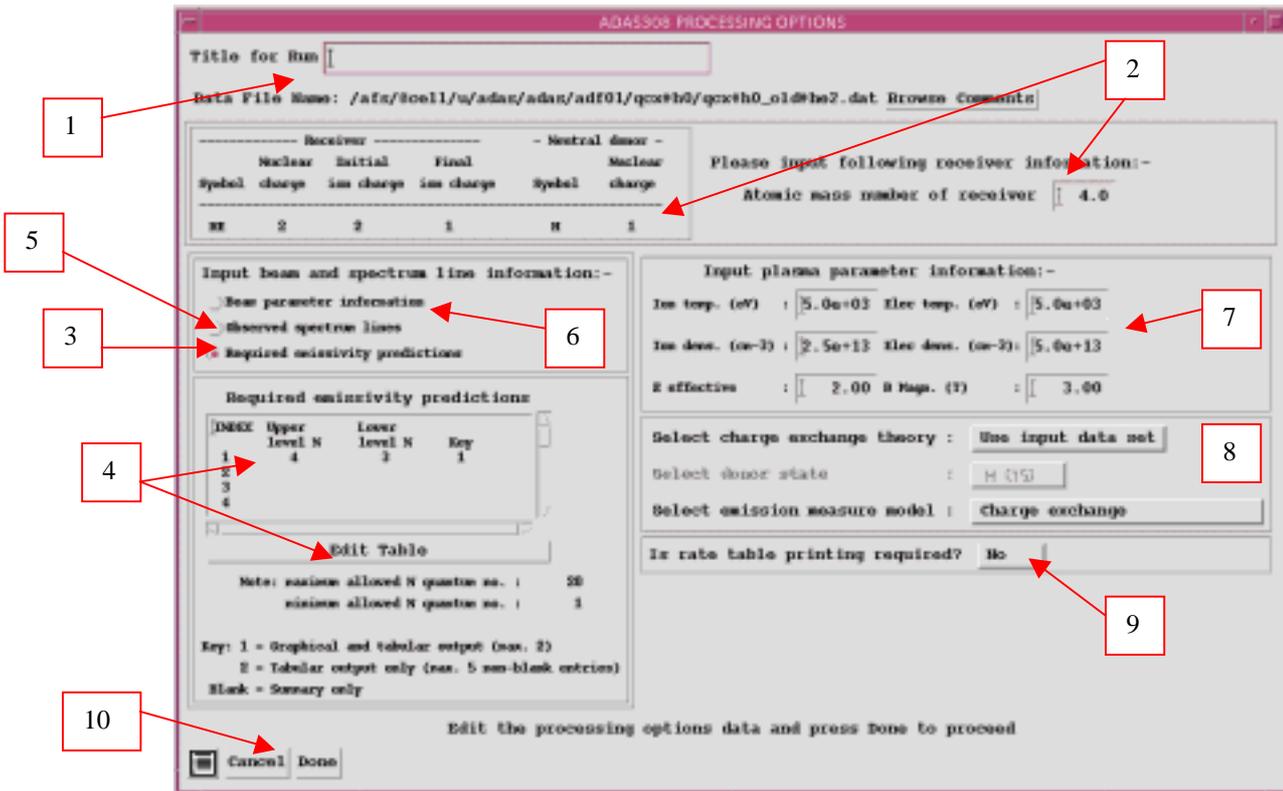5     Browse Comments  Cancel  Done

6. Clicking on the *Browse Comments* button displays any information stored with the selected datafile.  It is important to use this facility to find out what has gone into the dataset and the attribution of the dataset. The possibility of browsing the comments appears in the subsequent main window also.

7. Clicking the *Done* button moves you forward to the next window. Clicking the *Cancel* button takes you back to the previous window

The **processing options window** has the appearance shown below

1. An arbitrary title may be given for the case being processed.  For information the full pathway to the dataset being analysed is also shown.  The button *Browse Comments* again allows display of the information field section at the foot of the selected dataset, if it exists.

2. Information is given on the fully ionised impurity receiver and the neutral beam donor.  The atomic mass of the receiver must be entered.

3. The specification of beam parameters, details of observed line of sight spectral emissivities to be analysed and emissivities to be predicted are required.  Input data of each of these three types may be addressed in turn by activation of the relevant button.  The window below the button list  then presents the appropriate table.

4. *The Required emissivity predictions* button is displayed.  This activates the predictive part of the code which becomes possible once the observed lines have been analysed in terms of emission measure.  Then any set of lines within the N-shell limits may be predicted.  The standard output includes the mean wavelength and effective emison coefficient, but for up to five lines an extended tabulation of line component emissivities may be produced.  Graphs may be produced for two selected line.  Indicate these selections in the *Key* columnThe table may be edited by clicking on the *Edit Table* button.

5. The *Observed spectrum lines* table allows introduction of a number of observed intensities. It is possible to enter values which do not allow a consistent solution. The code advises of this but it is the responsibility of the user to check that the data is unblended etc. It is also a usual practice to enter just one line, possibly with a fictitious emissivity merely to obtain effective emission coefficients and line component details.

6. The *Beam parameter information* button causes display of the third editable table in the sub-window. Note that no check is made that the various beam energy fractions sum to unity. This is the responsibility of the user.



7. Enter the plasma environment parameters. These determine the collisional redistribution of the populations of the recombined plasma ion. For ADAS308, *B Magn*. has no effect, but a value should be entered as a place holder.

8. The final sub-window allows model and theory choices. Details are given in the ADAS Manual. For each type, clicking on the selection window drops down a short menu of choices. Click on the appropriate choice. The ADAS data base source numerical data of type ADF01 is the most usual, that is the *Use input data set* choice button. Note that the *Select emission measure* model choice includes *Electron impact excitation* as well *as Charge exchange*.

9. Extended information on the rates used in the populaiton modelling may be printed.

10. Clicking the *Done* button causes the next output options window to be displayed. Remember that *Cancel* takes you back to the previous window.

The **Output options window** is shown below. Note that two plots are produced if required. The *Plot A* is the stick diagram of component line-of-sight emissivities. The *Plot B* is of the Doppler broadened profile of the line at the plasma ion temperature.

1. As in the previous window, the full pathway to the file being analysed is shown for information. Also the *Browse comments* button is available.
2. Graphical display is activated by the *Graphical Output* button. This will cause a graph to be displayed following completion of this window. When graphical display is active, an arbitrary title may be entered which appears on the top line of the displayed graph. By default, graph scaling is adjusted to match the required outputs.
3. Press the *Explicit Scaling* button to allow explicit minima and maxima for the graph axes to be inserted. Activating this button makes the minimum and maximum boxes editable. Plot A axes limits refer to the 'stick diagram and Plot B axes limits to the Doppler broadened profile.
4. Hard copy is activated by the *Enable Hard Copy* button. The File name box then becomes editable A choice of output graph plotting devices is given in the Device list window. Clicking on the required device selects it. It appears in the selection window above the Device list window.
5. The *Text Output* button activates writing to a text output file. The file name may be entered in the editable File name box when *Text Output* is on. The default file name 'paper.txt' may be set by pressing the button *Default file name*.

The **Graphical output window** is shown below

1. Printing of the currently displayed graph is activated by the *Print* button.
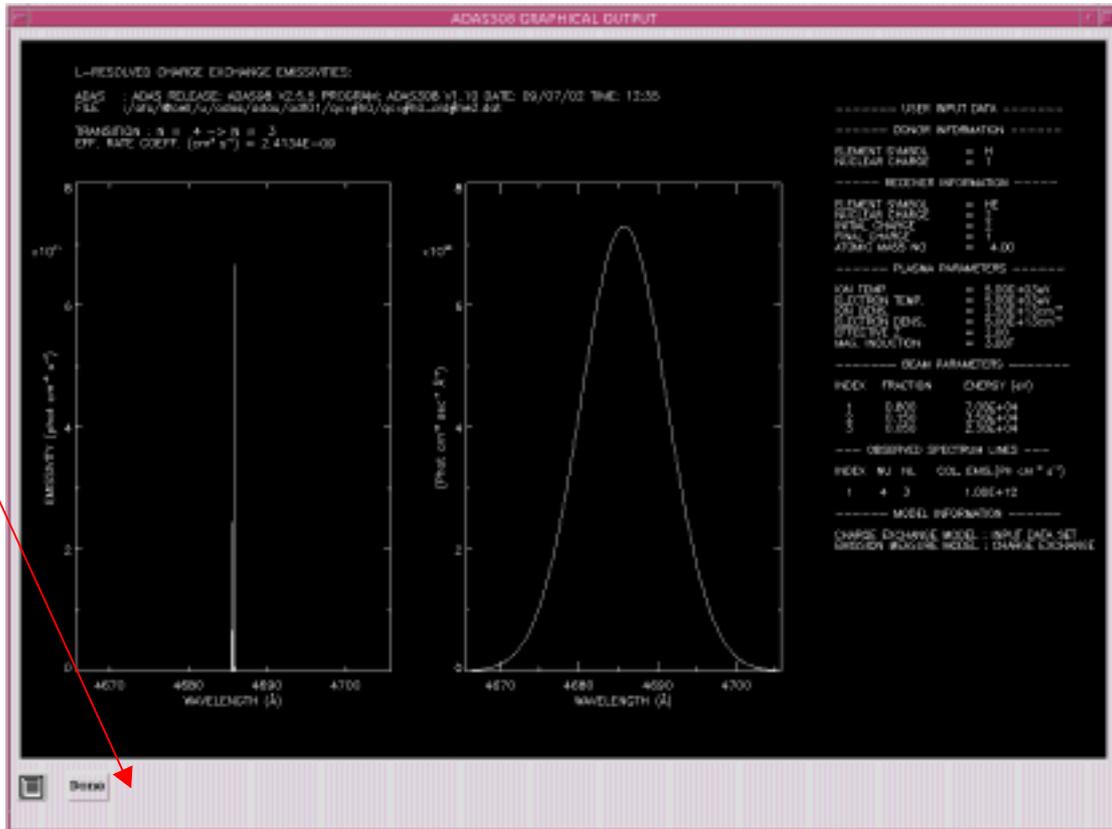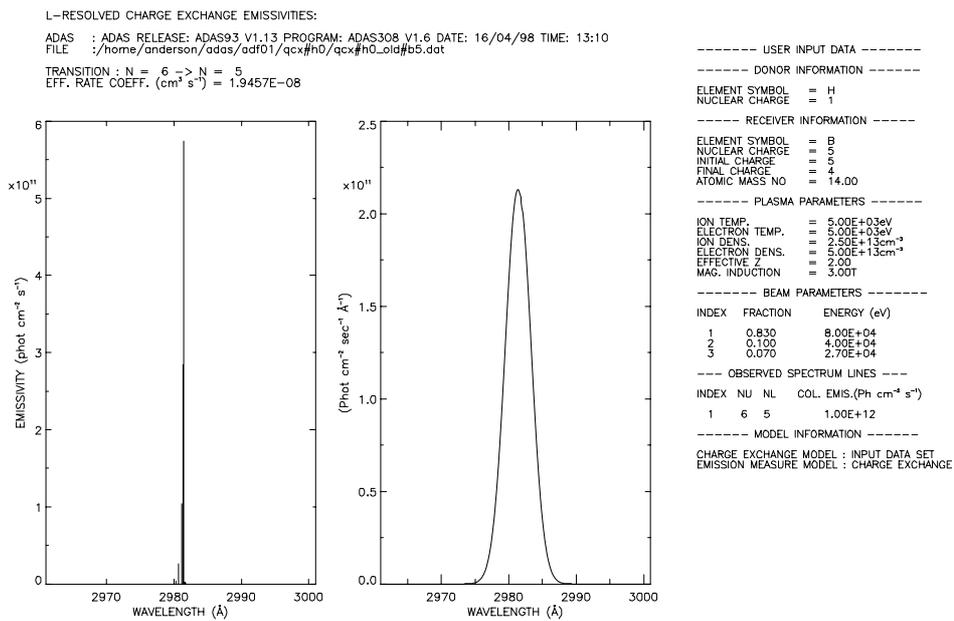


## Illustration:

.

Figure 4.8a

The analysis of charge exchange emission by the code is shown in figure 4.8a and table 4.8a. Emission following electron capture by $B^{+5}$ from neutral deuterium beam atoms in their ground state is illustrated. A single observed line-of sight emissivity in the transition BV (n = 6 ---> n = 5) is analysed. Figure 4.8a shows the theoretical breakdown of emission in the above line into multiplets and the expected Doppler broadened profile of the feature

Table 4.8a shows the tabular output. A detailed tabulation of the component photon fluxes is allowed for three spectrum line. In this case BV (n=6-5) is the 'observed line'. For the other selected charge exchange lines the predicted photon fluxes are computed using the calculated emission measure. The spectrum lines BV (n=5-4) and BV (n=4-3) are so tabulated.

Table 4.8a

```
ADAS RELEASE: ADAS93 V1.13 PROGRAM: ADAS308 V1.6 DATE: 16/04/98 TIME: 13:10
****** TABULAR INPUT  FROM       L-RESOLVED CHARGE EXCHANGE EMMISIVITY PROGRAM: ADAS308-DATE:16/04/98 *****

 ------------------                              ------------------
 FILE: /home/anderson/adas/adf01/qcx#h0/qcx#h0_old#b5.dat

                         RECEIVER      NEUTRAL DONOR
                         --------      -------------
 ELEMENT SYMBOL      =      B               H
 NUCLEAR CHARGE      =      5               1
 RECOMBINING ION CHARGE =   5               -
 RECOMBINED ION CHARGE  =   4               -
 ATOMIC MASS NUMBER  =   14.00              -

 PLASMA PARAMETERS:

  ION TEMPERATURE     (EV)  =   5.00D+03    ELECTRON TEMPERATURE (EV)  =   5.00D+03
  ION DENSITY       (CM-3) =   2.50D+13    ELECTRON DENSITY    (CM-3) =   5.00D+13
  PLASMA EFFECTIVE Z        =   2.00        MAGNETIC INDUCTION  (T)    =   3.00


 BEAM PARAMETERS:
  NUMBER OF BEAM COMPONENTS =  3

  INDEX    FRACTION        ENERGY
                            (EV)
  ------------------------------
    1       0.830        8.00D+04
    2       0.100        4.00D+04
    3       0.070        2.70D+04

 OBSERVED SPECTRUM LINES:
  NUMBER OF OBSERVED SPECTRUM LINES =  1

  INDEX   NU   NL     COL. EMIS.
                    (PH CM-2 SEC-1)
  ------------------------------
    1     6    5       1.00D+12

 CHARGE EXCHANGE MODEL : INPUT DATA SET
 EMISSION MEASURE MODEL: CHARGE EXCHANGE

  EMISSION MEASURE (CM-5) =   5.1394D+19

   N      QEX(N)        QTHEOR(N)
         (CM3 SEC-1)    (CM3 SEC-1)
  ------------------------------
   6    3.7316D-08    3.7316D-08
 ------------------------------------ PREDICTED EMISSIVITES ----------------------------------
  N  L    N1 L1    COL. POP.      COL. EMIS.              AIR WVLN.
                    (CM-2)       (PH CM-2 SEC-1)            (A)
  ---------------------------------------------------------------------
  6  0    5  1    1.0898D+01     1.8275D+09              2981.51
  6  1    5  2    2.3622D+01     1.4171D+09              2981.75
  6  1    5  0    2.3622D+01     3.5889D+09              2980.26
  6  2    5  3    9.3747D+01     2.2909D+09              2981.64
  6  2    5  1    9.3747D+01     2.6350D+10              2980.65
  6  3    5  4    2.3080D+02     1.6414D+09              2981.63
  6  3    5  2    2.3080D+02     1.0438D+11              2981.17
  6  4    5  3    4.1148D+02     2.8450D+11              2981.37
  6  5    5  4    5.5806D+02     5.7400D+11              2981.48
  ---------------------------------------------------------------------
  SUMS =     1.3286D+03     1.0000D+12   MEAN WVL(A) =   2981.39   EFF. RATE COEFFT. = 1.9457D-08
```

```
                         (CM-2)    (PH CM-2 SEC-1)                    (A)
        ----------------------------------------------------------------------
         5  0     4  1   1.7194D+01      6.9357D+09                 1619.35
         N  L     N1 L1  1COL510PDP1     COL63EMIS9                 AIR6WVLN2
         5  1     4  0   1.7510D+01      8.0720D+09                 1618.66
         5  2     4  3   9.6686D+01      3.0518D+09                 1619.48
         5  2     4  1   9.6686D+01      8.9831D+10                 1618.91
         5  3     4  2   3.0982D+02      5.0070D+11                 1619.22

         5  4     4  3   6.7088D+02      1.7847D+12                 1619.35
        ----------------------------------------------------------------------
        SUMS =    1.1121D+03     2.3953D+12   MEAN WVL(A) =   1619.30   EFF. RATE COEFFT. =  4.6607D-08

         N  L    N1 L1    COL. POP.     COL. EMIS.               AIR WVLN.
                         (CM-2)    (PH CM-2 SEC-1)                  (A)
        ----------------------------------------------------------------------
         4  0     3  1   4.5713D+01      5.2466D+10                 761.66
         4  1     3  2   1.8361D+01      3.9904D+09                 762.10
         4  1     3  0   1.8361D+01      3.5193D+10                 760.40
         4  2     3  1   1.2747D+02      5.6097D+11                 760.94
         4  3     3  2   5.1345D+02      4.4270D+12                 761.59
        ----------------------------------------------------------------------
        SUMS =    7.0500D+02     5.0796D+12   MEAN WVL(A) =    761.51   EFF. RATE COEFFT. =  9.8836D-08
        SUMMARY OF EMISSIVITIES:
         N   N1     COL. POP.      COL. EMIS.       AIR WVLN.     EFF. COEFFT.
                     (CM-2)     (PH CM-2 SEC-1)      (A)         (CM3 SEC-1)
        ----------------------------------------------------------------------
         6   5     1.3286D+03      1.0000D+12        2981.39      1.9457D-08
         5   4     1.1121D+03      2.3953D+12        1619.30      4.6607D-08
         4   3     7.0500D+02      5.0796D+12         761.51      9.8836D-08
```

# Notes: